Stress History of Soils from Cone Penetration Tests

P.W. Mayne

Abstract. Stress history is an important measurement in soils as it affects strength, stability, stiffness, and flow characteristics. The evaluation of the in-situ preconsolidation stress, or effective yield stress, from the results of piezocone penetration tests allows for an economical and expedient means to profile the stress history of clays, sands, and mixed soil types on geotechnical projects. The methodology is based on a derived analytical cavity expansion - critical state solution for clays and statistical inversion of data from calibration chamber tests on sands. Applications are given for case studies involving clay, silt, and sand where laboratory consolidation tests provide benchmark values for the stress history. Since yield stress demarcates contractive *vs.* dilative soil behavior, extended uses in screening soil susceptibility for concerns involving flow and cyclic liquefaction are also presented.

Keywords: clay, cone penetration, overconsolidation, piezocone, preconsolidation, sand, stress history, yield stress.

1. Introduction

The stress history of soils is a significant and important measure of its behavior in terms of stability, strength, deformational characteristics, and pore pressure behavior. The effective yield stress (σ_{vy}'), or preconsolidation stress ($\sigma_p' = P_c' = \sigma_{vmax}'$), represents the demarcation between normally-consolidated (NC) states and overconsolidated (OC) response. It also distinguishes the porewater pressures generated during shear which can either be positive or negative, and the volumetric strain characteristics that can be contractive or dilative.

Traditionally, the preconsolidation stress was defined as the maximum past stress that had been physically and mechanically applied to the soil, such as due to overburden erosion or glaciation. The more general term of effective yield stress ($\sigma_{vy}' = \sigma_p'$) has been recommended (*e.g.*, Leroueil & Barbosa 2000; Jardine *et al.*, 2003) since many other geological and environmental processes can result in a quasi-preconsolidation effect, such as ageing, cyclic loading, desiccation, repeated wetting-drying, groundwater changes, alternating freezing-thawing, bio-chemical bonding, etc.

2. Effective Yield Stress

The effective preconsolidation stress or yield stress of soils is best determined through a series of one-dimensional consolidation tests performed on undisturbed samples taken at different elevations in soil formation. A firm knowledge of the local engineering geology and terrain helps to put the stress history profile in a best perspective (Locat *et al.*, 2003). Figure 1 shows an example consolidation test conducted on a specimen of silty clay taken from a depth of 6.5 m at a highway embankment site in Evergreen, North Carolina (w = 70.8%, LL = 44%, PI = 19%). Results are plotted in terms of void ratio (e) *vs.* log of effective vertical stress (σ_v'), with a calculated in-situ effective overburden stress of σ_{vo}' = 43 kPa.

Using the classical construction technique from Casagrande (1936), a most probable magnitude of effective yield stress σ_p' = 80 kPa is determined. Following the orange dashed line, a minimum estimate of 65 kPa and maximum estimate of 90 kPa can also be extracted. Beyond this procedure, some 30 different graphical methods have been developed for the evaluation of σ_p' from consolidation test data (Ku & Mayne 2013).

The preconsolidation stress can be presented in dimensionless terms using a normalized form called the overconsolidation ratio (OCR), or the more generalized yield stress ratio (YSR), which is defined by:

$$\mathrm{YSR} = \frac{\sigma'_p}{\sigma'_{vo}} \tag{1}$$

The yield stress and YSR affect the behavior of soils and the magnitude of many geoparameters. A partial listing of the influence and significance of σ_p' and YSR is given in Table 1.

Another convenient parameter for representation of soil stress history is the yield stress difference, YSD, which is defined (Locat *et al.*, 2003):

$$\mathrm{YSD} = (\sigma'_p - \sigma'_{vo}) \tag{2}$$

The advantage of the YSD is that it is constant with depth for soil deposits that have become preconsolidated by erosion, glaciation, and/or excavation, where in contrast, the magnitude of YSR decreases with depth (Mayne 2007b). For soils that have a quasi-preconsolidation effect due to ageing, a constant YSR with depth is observed.

While oedometer and consolidometer tests will remain the benchmark for determining stress history profiles, there are often cases when "undisturbed" samples are diffi-

Paul W. Mayne, Ph.D., Professor, Civil & Environmental Engineering, Georgia Institute of Technology, 790 Atlantic Drive, 30332-0355 Atlanta, GA, USA. e-mail: paul.mayne@ce.gatech.edu.
Invited Lecture, no discussions.
DOI: 10.28927/SR.403203

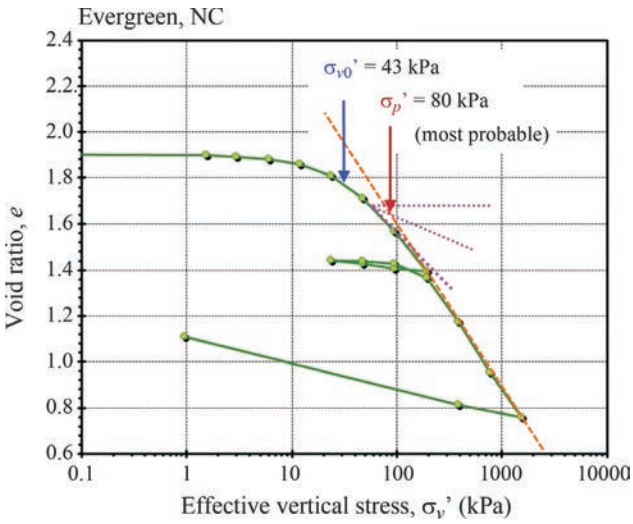

Figure 1 - Post-processing consolidation test results on clay from Evergreen, North Carolina for evaluating yield stress.

cult to procure because of the silty to sandy nature of the ground, inevitable sample disturbance, ageing and storage effects, and stress relief, as well as the expense and necessary time required for laboratory testing. Therefore, it has become of great interest and motivation in seeking in-situ test based methods to evaluate stress history profiles of soils, specifically using the cone penetration test (CPT) and piezocone (CPTu). These acquired data can be used to complement the laboratory program and fill in gaps between sampling depths and locations.

The interpretation of a full suite of geoparameters using CPT and CPTu is detailed elsewhere (Robertson 2009; Schnaid 2010; Mayne 2015).

3. Analytical SCE-CSSM Model for CPTU in Clays

A hybrid analytical model for piezocone penetration in clays was developed from Spherical Cavity Expansion (SCE) theory and Critical State Soil Mechanics (CSSM), as detailed by Mayne (1991, 2005) and Chen & Mayne (1994). The SCE-CSSM formulation provides for separate evaluations for the YSR in terms of the net cone resistance ($q_{net} = q_t - \sigma_{vo}$) and/or the measured excess porewater pressure ($\Delta u = u_2 - u_0$):

$$\text{YSR} = 2\left[\frac{\dfrac{q_t - \sigma_{vo}}{\sigma'_{vo}}}{M\left[\dfrac{2}{3}(\ln I_R + 1) + \dfrac{\pi}{4} + \dfrac{1}{2}\right]}\right]^{\frac{1}{\Lambda}} \quad (3)$$

$$\text{YSR} = 2\left[\frac{\dfrac{\Delta u}{\sigma'_{vo}} - 1}{\dfrac{2}{3} M \ln(I_R) - 1}\right]^{\frac{1}{\Lambda}} \quad (4)$$

where $M = 6\sin\phi'/(3 - \sin\phi')$ = frictional envelope in Cambridge University type q - p' space, $I_R = G/s_u$ = undrained rigidity index, G = shear modulus, s_u = undrained shear strength, and $\Lambda = 1 - C_s/C_c$ = plastic volumetric strain potential, with C_s = recompression or swelling index, and C_c = virgin compression index. The value of $\Lambda \approx 0.8$ for most clays (Ladd & DeGroot 2003).

For soft to firm clays, the shear-component of porewater pressures is small (< 20%) of the total measured porewater pressures (Baligh 1986; Burns & Mayne 2002). Thus, neglecting that component, Eq. (4) can be reduced without much error to:

$$\text{YSR} = 2\left[\frac{\dfrac{\Delta u}{\sigma'_{vo}}}{\dfrac{2}{3} M \ln(I_R)}\right]^{\frac{1}{\Lambda}} \quad (5)$$

Finally, by combining Eqs. (3) and (4), a third estimate of OCR can be formulated in terms of effective cone

Table 1 - Importance of yield stress and YSR = σ_p'/σ_{vo}' on soil behavior and geoparameters.

Geoparameter or behavioral facet	Relevance
Degree of overconsolidation	Separates normally-consolidated (NC) and overconsolidated (OC) regions
Settlement analysis	Demarcates recompression from virgin compression on consolidation: e-log σ_v'
Undrained shear strength	$s_u/\sigma_{vo}' = 1/2\sin\phi' \text{YSR}^{\Lambda}$ where $\Lambda = 1 - C_s/C_c$ and ϕ' = friction angle
Geostatic lateral stress	$K_0 = (1 - \sin\phi')\text{YSR}^{\sin\phi'}$
Porewater pressures	Skempton's parameter A_f
Anchors the yield surface	Constitutive soil models
Elastic soil moduli	E' and E_u
Small-strain stiffness	$G_{max} = F(e)\ p'\ \text{YSR}^k$ where $F(e)$ = void ratio function p' = effective stress and k = plasticity effect
Screening for flow liquefaction of soils	Alternate to state parameter (ψ) separating contractive *vs.* dilative response
Screening for cyclic liquefaction potential	Supplement to CSR and CRR

resistance ($q_E = q_t - u_2$) that removes the reliance on rigidity index (I_R):

$$YSR = 2\left[\frac{1}{1.95M+1}\left(\frac{q_t - u_2}{\sigma'_{vo}}\right)\right]^{\frac{1}{\Lambda}} \quad (6)$$

The above equations can be simplified from power law expressions to form linear equations for evaluating effective yield stress in intact clays. Adopting a value $\Lambda = 1$, the three CPTu formulae given by Eqs. (3), (5), and (6) are reduced to:

$$\sigma'_p = \frac{q_t - \sigma_{vo}}{M(1 + \frac{1}{3}\ln I_R)} \quad (7)$$

$$\sigma'_p = \frac{u_2 - u_0}{\frac{1}{3} M \ln I_R} \quad (8)$$

$$\sigma'_p = \frac{q_t - u_2}{0.957M + 0.5} \quad (9)$$

3.1. Case study – Hartford, Connecticut

Geotechnical investigations for a five-story hotel in Hartford, Connecticut included soil borings and series of seismic piezocone tests (SCPTu) for settlement and bearing capacity analyses of shallow spread footings. The site is located adjacent to the Connecticut River and a representative SCPTu is shown in Fig. 2. The profile indicates an upper 11.5 m thick sand stratum underlain by a firm clay that extends to about 26 m. Lab data from the nearby Bissell Bridge are available (Long *et al.*, 1978), with a summary of drained and undrained triaxial compression tests indicating

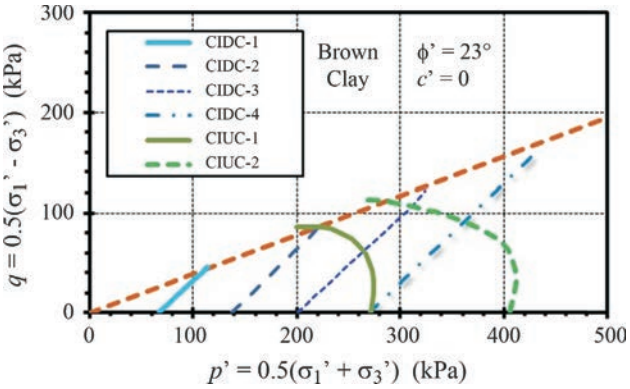

Figure 3 - Effective stress paths for CIDC and CIUC tests on brown clay at Bissell Bridge, Hartford, Connecticut (data from Long *et al.*, 1978).

an effective stress friction angle ϕ' = 23° for the brown clay, as presented in Fig. 3. The SCPTu results can be used to estimate the rigidity of the clay (G taken at 50% of strength) from a recent formulation developed by Krage *et al.* (2014):

$$(I_R)_{50} = \frac{1.81 G_0}{(q_{net})^{0.75}(\sigma'_{vo})^{0.25}} \quad (10)$$

where $G_0 = \rho_T V_s^2$ is the small-strain shear modulus and ρ_T = total soil mass density. For the current data, an average value of $I_R = 127$ was obtained.

Using Eqs. (7), (8), and (9) with ϕ' = 23° and $I_R = 127$ gives the three separate and corresponding profiles of yield stress and YSR shown in Fig. 4. These agree well with the results of one-dimensional consolidation tests reported by Long *et al.* (1978).

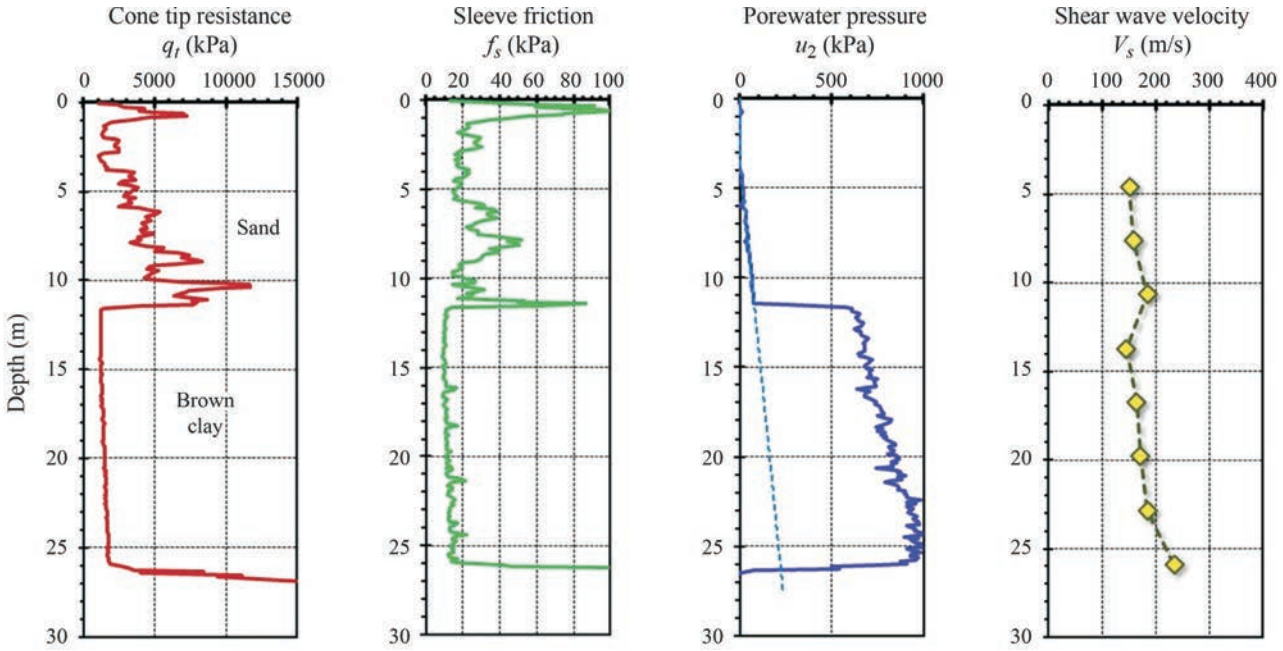

Figure 2 - Representative seismic piezocone sounding at site in Hartford, Connecticut.

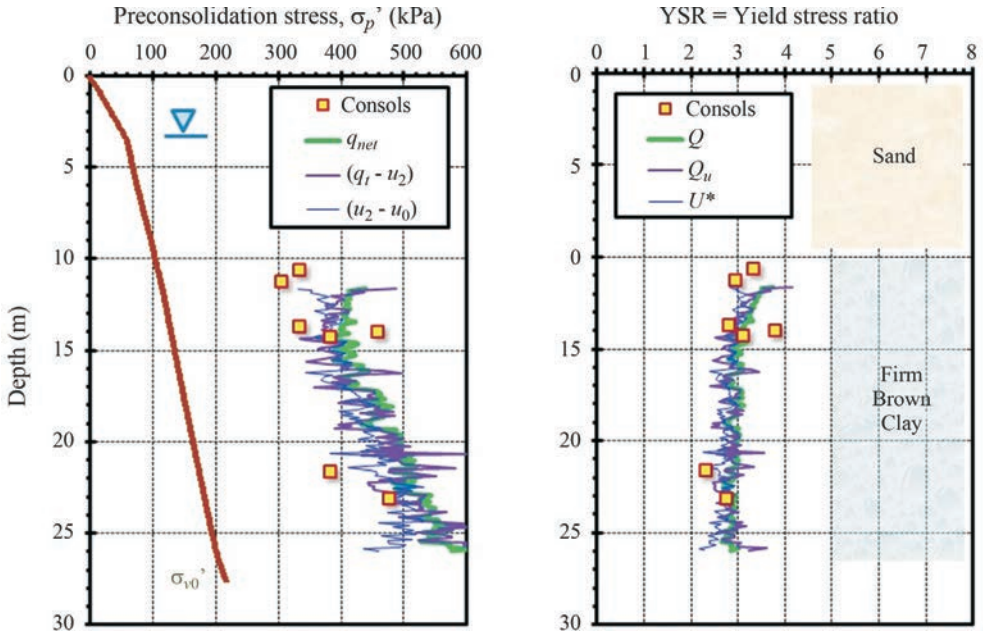

Figure 4 - Profiles of effective yield stress and YSR from consolidation tests and SCPTu at Hartford site.

3.2. Yield stresses from CPTU in soft inorganic clays

The full range for measured effective stress friction angle of natural clays is in the range $17° \leq \phi' \leq 43°$ (Diaz-Rodriguez *et al.*, 1992). A review of triaxial data from 453 clays indicates a mean $\phi' = 28.6°$ with standard deviation S.D. ± 5.0° (Mayne 2013). Ranges of the rigidity index are much larger, yet the SCE-CSSM expressions are a function of $\ln(I_R)$, so much more forgiving in exactitude. Shear modulus is highly nonlinear from the nondestructive range at G_0 to intermediate values at medium strains (G) and low values at peak strength (Viana da Fonseca *et al.*, 2011). Full ranges of laboratory-measured rigidity indices for soft clays is reported as: $40 \leq I_R \leq 600$ that decreases with increasing YSR (Casey *et al.*, 2016). A default value is often taken as $I_R = 100$ (*e.g.*, Teh & Houlsby 1991).

For intact inorganic clays of low sensitivity and low OCR < 3, the SCE-CSSM expressions can be further simplified for practical use by adopting characteristic values of $\phi' = 30°$ and $I_R = 100$ (Mayne 2001, 2005):

$$\sigma'_p = 0.33(q_t - \sigma_{vo}) \quad (11)$$

$$\sigma'_p = 0.54(u_2 - u_o) \quad (12)$$

$$\sigma'_p = 0.60(q_t - u_2) \quad (13)$$

Of course, these coefficients should be adjusted based on local geologies and site-specific geomaterials, where possible.

These relationships have been studied for a wide variety of clays, including statistical studies involving: 206 different sites (Chen & Mayne 1996); 22 sites in Canada (Demers & Leroueil 2002); 17 Norwegian clays (Karlsrud *et al.*, 2005); as well as individual sites, *e.g.*, Pisa, Italy (Jamiolkowski & Pepe 2001); Costa Rica (Eller *et al.*, 2014). Results from Swedish clays give similar values however the coefficients appear to trend with plasticity index (Larsson & Mulabdic 1991; Larsson & Åhnberg 2005), whereas the study involving clays of eastern Canada did not show such a trend (Demers & Leroueil 2002).

3.3. Soft clay at Torp, Sweden

For soft intact clays, it is warranted to utilize all three equations, as redundancy can be helpful in geotechnical site characterization. If the three methods show consensus, then this helps to validate a "well-behaved" clay and encourages further use of these relationships in the geological setting. An illustrative application of all three solutions given by Eqs. (11), (12), and (13) is given in Fig. 5 for a soft clay site in Torp, Sweden (Larsson & Åhnberg 2003). The estimated profiles of σ_p' and YSR from the CPTu-estimates compare well with the rather large set of consolidation test results at this site.

If the three methods show disparities, then a closer examination and scrutiny of the laboratory and/or field data may be warranted, perhaps providing justification that additional testing and investigation should be conducted. lf unusual mineralogy exists in the soil (*i.e.*, calcite, diatoms, forams, etc.), it may be possible to re-tune these equations for the particular geologic formation attributes (*e.g.*, Mayne 2005).

In highly sensitive or structured clays, it has been recognized that Eq. (11) gives a slight underprediction in the σ_p' profile, while a serious overestimation occurs with Eq. (12) and a large underestimate when using Eq. (13). For clays with a very pronounced strain-softening after peak in

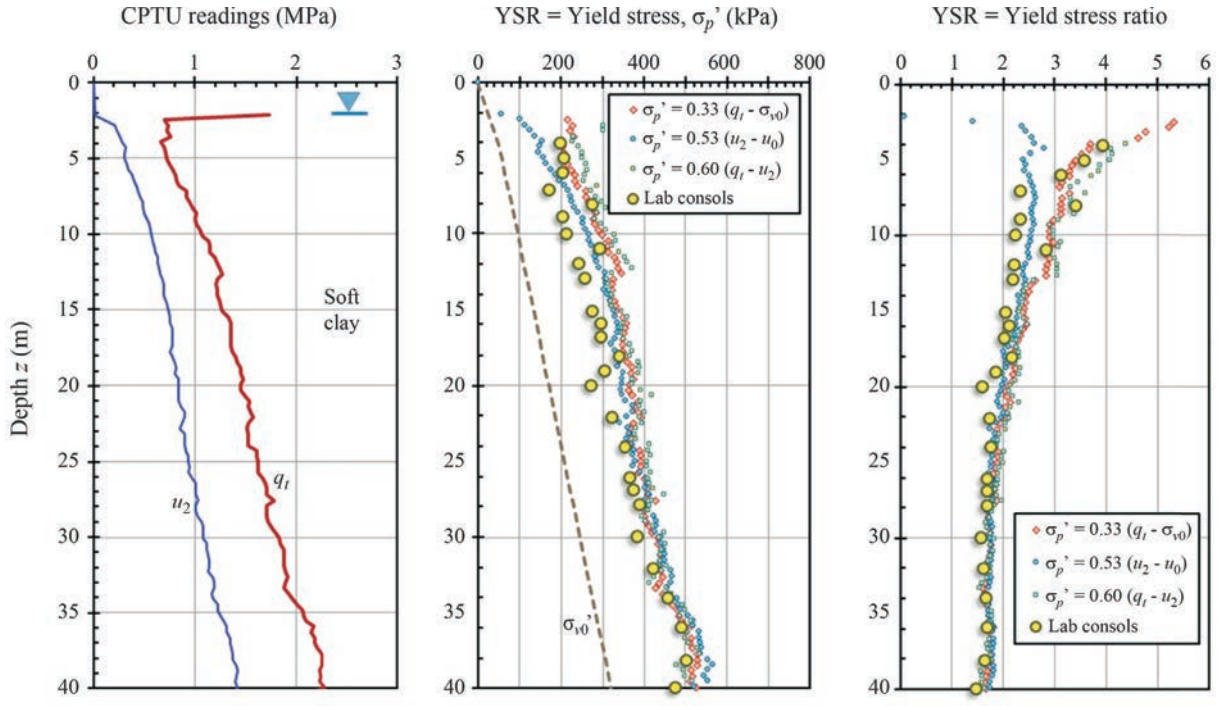

Figure 5 - CPTu data and YSR evaluations for Torp clay, Sweden (data from Larsson & Åhlberg 2003).

their stress-strain-strength behavior, a modified SCE-CSSM is available (Agaiby & Mayne 2018).

3.4. Yield stresses in organic clays using CPTu

The fitted coefficients in Eqs. (11), (12), and (13) for a number of soft organic clays in Brazil are reportedly quite different (Coutinho & Bello 2014). For instance, 0.125 q_{net} and 0.154 q_E are recommended (Baroni & Almeida 2017). This may reflect either a higher operational value of friction angle and/or rigidity index than the above adopted "characteristic" values used in the SCE-CSSM solution, or perhaps can be related to the organic content and mineralogy of these clays. An adjustment for the coefficients is necessary for the organic sulfide clays of Sweden (Larsson *et al.*, 2007). Here, the normal coefficients (0.33, 0.53, 0.60) are better fitted with values (0.22, 0.68, 0.28).

In lieu of adjusting the coefficients, an alternative approach to addressing σ_p' in organic clays is offered in the Section 5 of this paper.

4. Yield Stress Evaluation in Sand from CPT

A statistical review of over 626 calibration chamber tests on 26 different clean sands of silica and quartz constituency has been compiled (Mayne 2001). By inversion, this study determined relationships between the measured net cone resistance (q_{net}) and the applied stress state, including effective vertical stress (σ_{vc}'), lateral stress ratio ($K_0 = \sigma_{vc}'/\sigma_{vc}'$), and induced OCR, as summarized in Fig. 6. A direct expression for evaluating the YSR in clean sands is given by (Mayne 2005):

$$\text{YSR} = \left[\frac{0.192 \left(\frac{q_{net}}{\sigma_{atm}} \right)^{0.22}}{(1 - \sin\phi') \left(\frac{\sigma'_{vo}}{\sigma_{atm}} \right)^{0.31}} \right]^{\frac{1}{\sin\phi' - 0.27}} \quad (14)$$

Taking a characteristic value of friction angle $\phi' = 35.5°$ for clean sands, Eq. (14) reduces to the linear format:

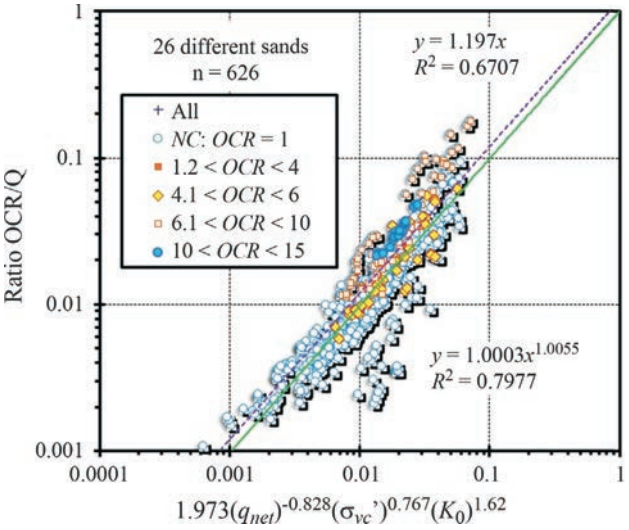

Figure 6 - Inversion relationship from CPT chamber tests on 26 different quartz-silica sands.

$$\sigma'_p = 0.08 q_{net}^{0.7} \sigma_{atm}^{0.3} \quad (15)$$

Using SI units, the reference stress is σ_{atm} = 1 bar = 100 kPa, therefore Eq. (15) further diminishes to the even simpler expression:

$$\sigma'_p = 0.32 q_{net}^{0.7} \text{ (units of kPa)} \quad (16)$$

which bears an uncanny resemblance to the expression for clay given by Eq. (11). As shown by Fig. 7, the simplified approach for clean sands compares well with the more rigorous algorithm given by Eq. (14) for the specified ranges of ϕ', stress level (σ_{vc}'), and normalized cone resistance. For high stress levels and high values of ϕ', the simplified approach will underpredict the yield stresses.

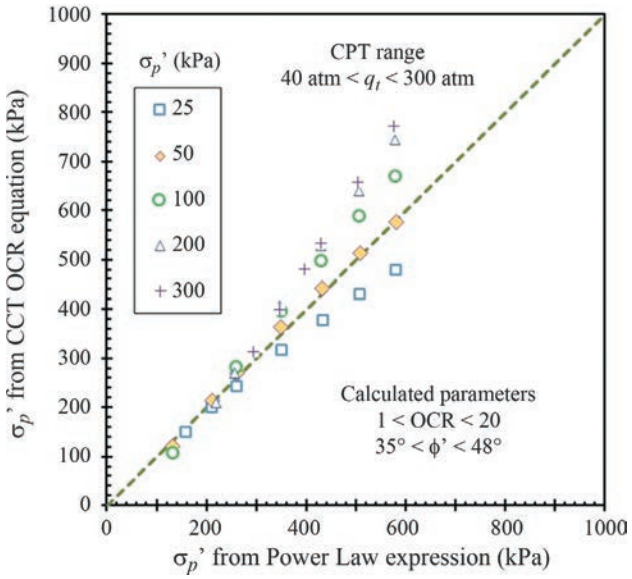

Figure 7 - Comparison of yield stress of sands from statistical algorithm and simplified solution.

4.1. Case study from Blessington Sand Site, Ireland

The aforementioned approach can be applied to a case study involving dense OC sands in Blessington, Ireland (Doherty *et al.*, 2012). The site is used by Univ. College Dublin for offshore pile research (Gavin *et al.*, 2013). The glacially-derived dense fine sands have an in-place relative density around 100% and mean particle size: 0.10 < D_{50} (mm) < 0.15 mm. Mineralogies include a predominance of quartz with calcite component, and subsets of feldspar, mica, and kaolinite fractions.

Measured cone tip resistances from 4 CPT soundings at the test site are presented in Fig. 8a. Samples of the sand were procured using sonic drilling methods that were later tested in the laboratory consolidometer to define the yield stress (σ_p') per Casagrande method. The interpreted profiles of yield stress from the simplified CPT approach are shown in Fig. 8b along with a comparison to the lab reference values, with good agreement evident.

5. Generalized Profiling of YSR by CPT

For the general case of evaluating effective yield stress in all soil types, Fig. 9 provides a compilation of data from a variety of natural formations, including sands, silts, clays, and mixed geomaterials. The independent expres-

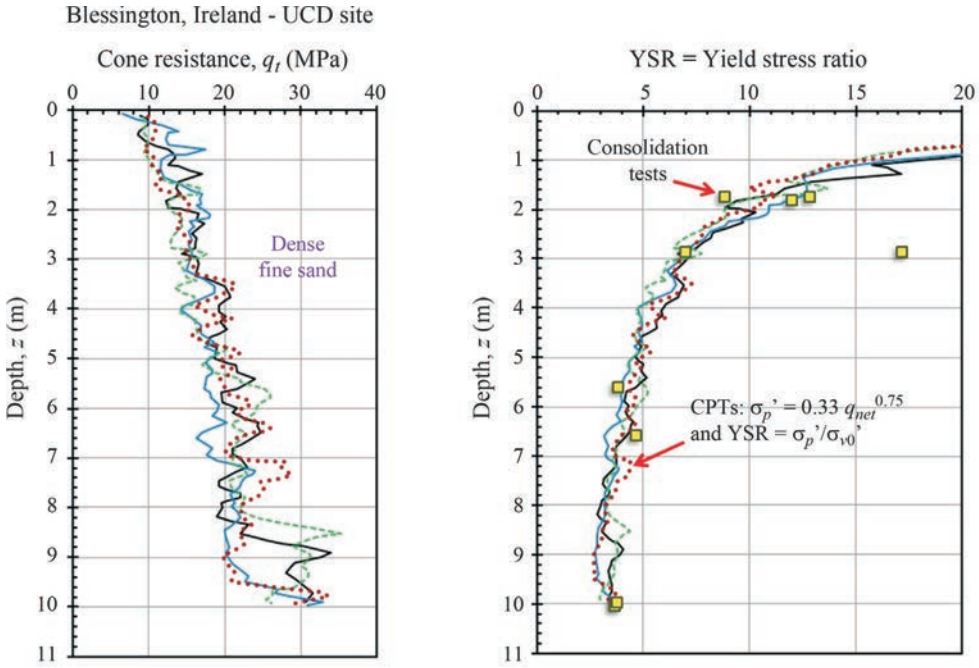

Figure 8 - Profiles of cone resistance and yield stress ratio in dense overconsolidated sands at Blessington, Ireland (data from Doherty *et al.*, 2012).

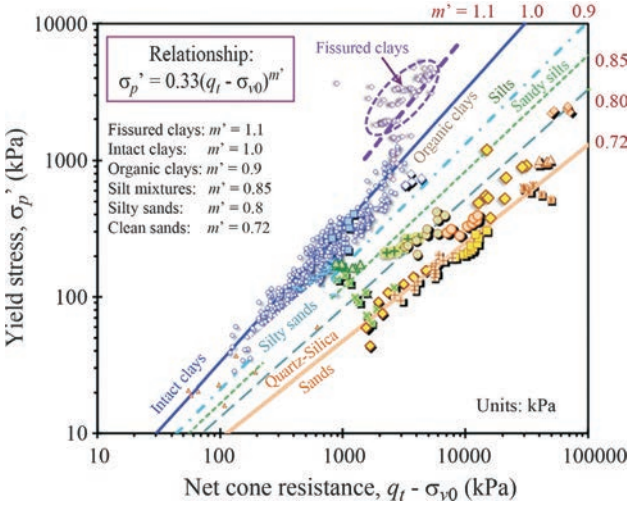

Figure 9 - Yield stress *vs.* net cone resistance for wide range of geomaterials (after Mayne, Coop, Springman, Huang, and Zornberg 2009).

sions for clays and sands can be united to provide the general format:

$$\sigma'_p = 0.33(q_t - \sigma_{vo})^{m'} \left(\frac{\sigma_{atm}}{100} \right)^{1-m'} \quad (17)$$

where the exponent m' increases with fines content and decreases with mean grain size. Specifically, the value of $m' \approx 0.72$ in clean quartz sands, 0.8 in silty sands, 0.85 in silts, and is 1.0 in intact clays of low sensitivity. It may even take on values of 1.1+ in fissured geomaterials. If only SI units are used (kPa), the form simply becomes:

$$\sigma'_p = 0.33(q_t - \sigma_{vo})^{m'} \text{ (in kPa)} \quad (18)$$

For soft organic clays, it appears the exponent takes on value of around $m' = 0.9 \pm 0.1$, thus site-specific calibrations will be required when working with these soils. As indicated in Section 3.5, an alternate approach is to adopt $m' = 1$ and employ a lower coefficient.

5.1. Yield stress exponent from CPT material index

The CPT material index I_c is used to evaluate soil behavioral type from cone penetrometer readings in natural soil formations (*e.g.*, Riyis & Giacheti 2017), mine tailings (Schnaid *et al.*, 2014), and soil liquefaction assessment (Rodrigues *et al.*, 2016). Details are given by (Robertson 2009) where the index is determined by:

$$I_c = \sqrt{(3.47 - \log Q_{tn})^2 + (1.22 + \log F)^2} \quad (19)$$

where Q_{tn} = normalized cone resistance that is defined by:

$$Q_{tn} = \frac{\frac{q_t - \sigma_{vo}}{\sigma_{atm}}}{\left(\frac{\sigma'_{vo}}{\sigma_{atm}} \right)^n} \quad (20)$$

and the normalized sleeve friction (F) is determined from:

$$F(\%) = \frac{100\, f_s}{q_t - \sigma_{vo}} \quad (21)$$

The exponent "n" varies from 1 in intact clays to around 0.5 in sands. It is specifically determined from (Robertson 2009):

$$n = 0.381 I_c + 0.05 \left(\frac{\sigma'_{vo}}{\sigma_{atm}} \right) - 0.05 \leq 1.0 \quad (22)$$

Thus, an iterative solution is needed to find I_c. In terms of soil classification, sands are identified when $I_c < 2.05$ while clays are found when $I_c > 2.95$. Intermediate soil types to these values include sandy mixtures and silty mixtures that are separated at $I_c = 2.60$, which is also the threshold for soil behavior: *i.e.*, drained when $I_c < 2.60$ and undrained when $I_c > 2.60$.

The material index I_c also provides a means of quantifying the magnitude of the yield stress exponent m' for the automatic CPT profiling of σ_p' in homogeneous soils, heterogeneous deposits, mixed geomaterials, and stratified formations. Figure 10 shows the trend between m' and CPT index (I_c) given by:

$$m' = 1 - \frac{0.28}{1 + \left(\frac{I_c}{2.65} \right)^{25}} \quad (23)$$

Where possible, the interpreted σ_p' results should be cross-checked and validated with other information, such as the results from one-dimensional consolidation tests on high-quality undisturbed samples, as well as the geologic stress history. In certain cases, additional results and corroboration may be obtained by running other in-situ tests, such as the flat plate dilatometer test (DMT) and/or vane shear test (VST), as discussed elsewhere (Schnaid 2009).

5.2. British Columbia

A representative SCPTu sounding shows a stratified soil profile from the Golden Ears Bridge south of Vancouver, British Columbia in Fig. 11 (Niazi *et al.*, 2010). The profile indicates silty to sandy layers that occupy the upper 40 m and overlie deeper deposits of clays to sensitive clays that extend to at least 95 m below grade. The sand-clay demarcation is evident from the change in porewater pressures readings at around 40 m, as well as the CPT material index profile shown in Fig. 12. Yet despite the abrupt transitions from silts to sands to clays, the post-processing of the CPT data in these geologically-related Holocene units

shows a consistent and gradual yield stress profile indicating lightly-overconsolidated sediments with low YSRs. Although no lab consolidation tests were available, estimated yield stresses from shear wave velocity measurements (Mayne 2005) confirm the low values of YSR ≈ 1.5, as shown by Fig. 12.

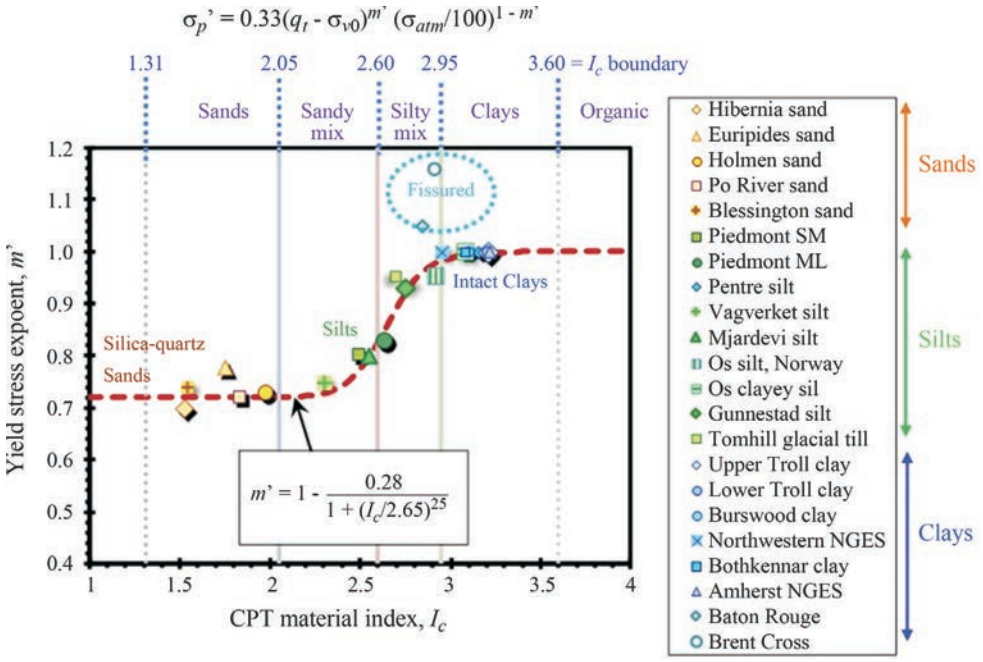

Figure 10 - Exponent m' for yield stress evaluation *vs.* CPT material index in non-cemented quartz-silica sands and inorganic clays of low sensitivity.

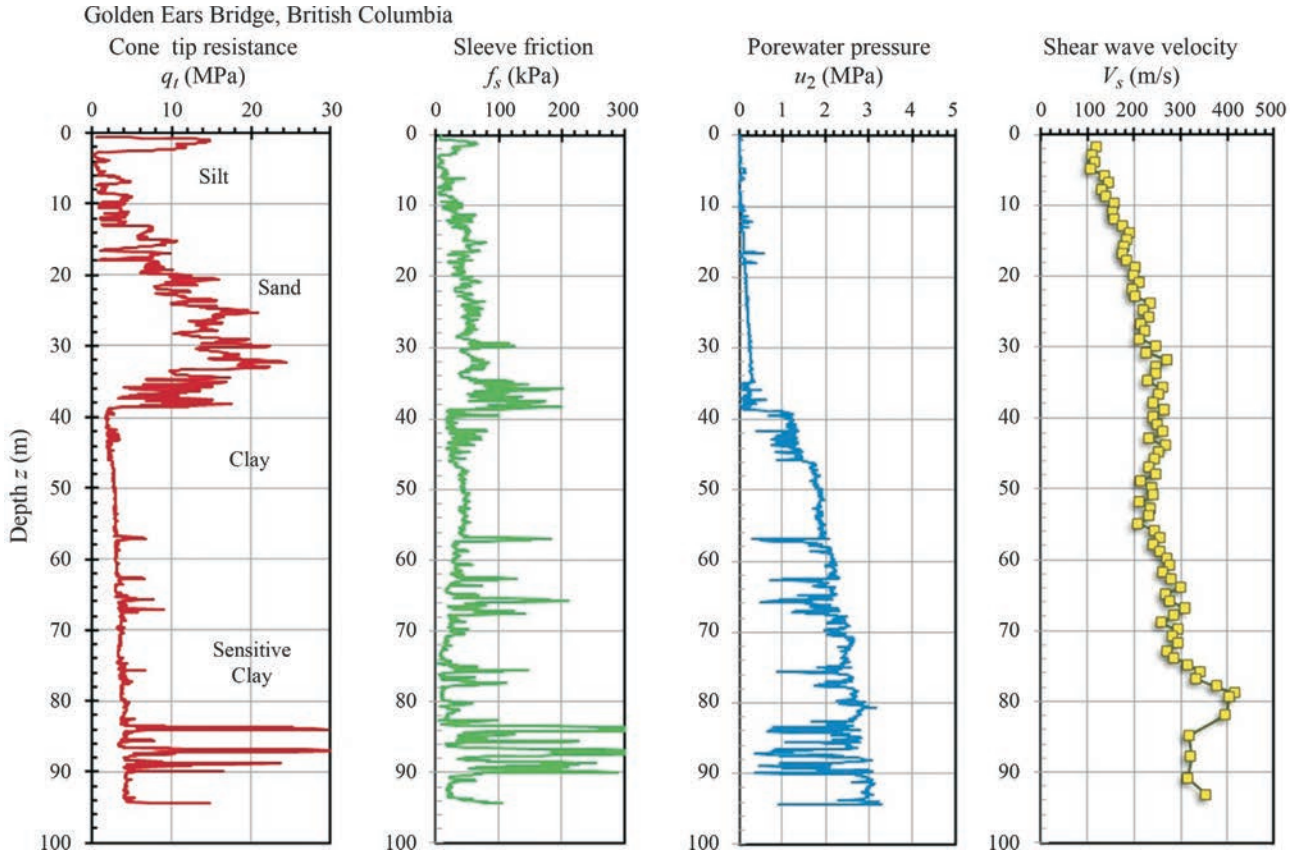

Figure 11 - Representative SCPTu at Golden Ears Bridge, BC (Niazi *et al.*, 2010).

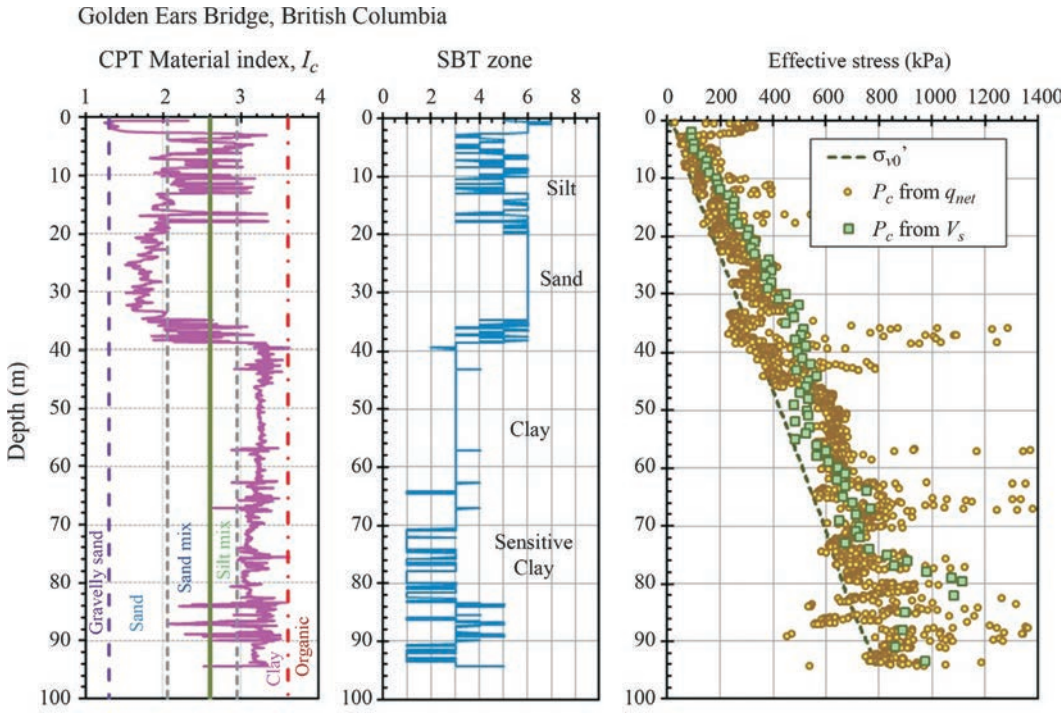

Figure 12 - Interpreted profiles at Golden Ears Bridge: (a) CPT material index; (b) soil behavioral type; and (c) effective yield stresses.

6. Soil Liquefaction

Two primary concerns in soil dynamics include: (a) flow liquefaction associated with mine tailings and dam stability; and (b) cyclic liquefaction caused by earthquakes. For both topics, critical state soil mechanics (CSSM) provides a rational and useful framework for the understanding and evaluation of soils that are prone to liquefaction (Viana da Fonseca 2011).

The approach to using CSSM for flow and cyclic liquefaction in sands has been via use of the state parameter: $\psi = e_0 - e_{CSL}$, where e_0 = initial in-situ void ratio and e_{CSL} = void ratio at critical state for constant effective stress (Jefferies & Been 2006; Idriss & Boulanger 2008). Sands that are prone to liquefaction are contractive and have a characteristic $\psi > 0$, while in contrast, dilative sands are not so susceptible and exhibit $\psi < 0$. The value of $\psi = 0$ is therefore a theoretical screening value, however, often a threshold $\psi = -0.05$ has been adopted for practical purposes and conservative benchmark (Robertson 2010).

While ψ works well, the methodology can be alternatively represented in terms of YSR just as effectively. Herein, we shall explore its vantages within a simplified version of CSSM (Mayne *et al.*, 2009; Holtz *et al.*, 2011). As presented in Fig. 13, the critical state line (CSL) can be represented in terms of ψ as a drained stress path, or alternately as an equivalent YSR, termed YSR_{CSL}. In fact, YSR and ψ have been interrelated through their compressibility parameters (C_c, C_s) and frictional properties (ϕ'), as shown by Been *et al.* (1988) and Plewes *et al.* (1992).

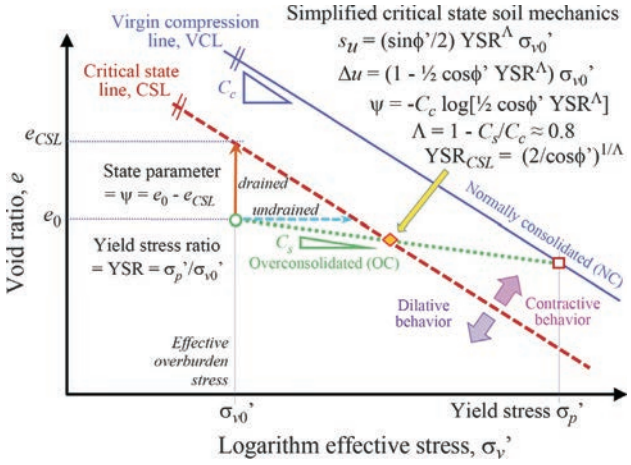

Figure 13 - Simplified critical state soil mechanics and definition of state parameter.

For the mode of simple shear, simplified CSSM provides the magnitude of excess porewater pressures during undrained shearing:

$$\Delta u = (1 - \tfrac{1}{2}\cos\phi' \cdot YSR^{\Lambda})\sigma'_{vo} \quad (24)$$

For clays, a characteristic value of $\Lambda = 0.80 \pm 0.10$ is well recognized (Ladd & DeGroot, 2003). Compressibility parameters for various sands were reviewed by Been *et al.* (1987) including Monterey, Ticino, Hokksund, Ottawa, Reid Bedford, and Hilton Mines. The measured C_c and C_s values indicate an overall mean $\Lambda = 0.790$ with S.D. = 0.164 (n = 24) for these sands. Thus, the value of

$\Lambda = 0.80$ can be considered characteristic for soils in general.

The boundary separating contractive and dilative soil behavior is defined when $\Delta u = 0$ during undrained shear. The corresponding YSR at critical state is then calculated as:

$$YSR_{CSL} = \left(\frac{2}{\cos \phi'} \right)^{\frac{1}{\Lambda}} \quad (25)$$

Analogous to the ψ threshold, this YSR_{CSL} becomes the threshold for identifying contractive unstable soils from those that are dilative and rather stable (Mayne *et al.*, 2017). In fact, Robertson (2012) suggested that a YSR = 4 was a reasonable threshold for this purpose.

For purposes of calculating the yield stress ratio at the critical state, the following equations can be recommended for the effective friction angle (Mayne 2007a):

when $I_c < 2.6$,

$$\phi' = 17.6° + 11.0° \log (Q_{tn})$$

when $I_c > 2.6$,

$$\phi' = 29.5° B_q^{0.121} [0.256 + 0.336 B_q + \log(Q_{tn})]$$

6.1. Flow liquefaction example - tailings

At a gold mine facility (site A) in western USA, results from the processing of a representative CPTu sounding in tailings comprised of sandy silts are presented in Fig. 14 (Been *et al.*, 2012). Adjacent soil borings with sampling, and laboratory testing indicated that most recovered samples had fines contents (FC) ranging from 45% to 75%, generally FC > 50%. Per the Unified Soil Classification System (USCS), these tailings are predominantly low-plasticity sandy silts (ML) with clay fractions (CF < 0.002 mm) less than 10%. In addition to the q_t profile in Fig. 14a, the soil behavioral type classification system using the CPT material index (I_c) is shown in Fig. 14b, indicating primarily silty mixtures with mixed sandy zones, in agreement with the borings and lab results.

The interpreted yield stresses are generally just above the current effective overburden stresses, thus these geomaterials are normally- to lightly-overconsolidated (NC to LOC). At depths > 3 m, Fig. 14c shows the YSR profiles are generally below 3 and thus contractive over the rest of the sounding to 22 m. This agrees well with the more elaborate CPT analysis for state parameter (Been *et al.*, 2012) shown in Fig. 14d, clearly showing a $\psi > -0.05$ over most of the profile.

6.2. Cyclic liquefaction example - Christchurch

The same procedure using a threshold YSR_{CSL} to separate contractive *vs.* dilative soils can be implemented for screening cyclic liquefaction susceptibility (Mayne & Styler 2018).

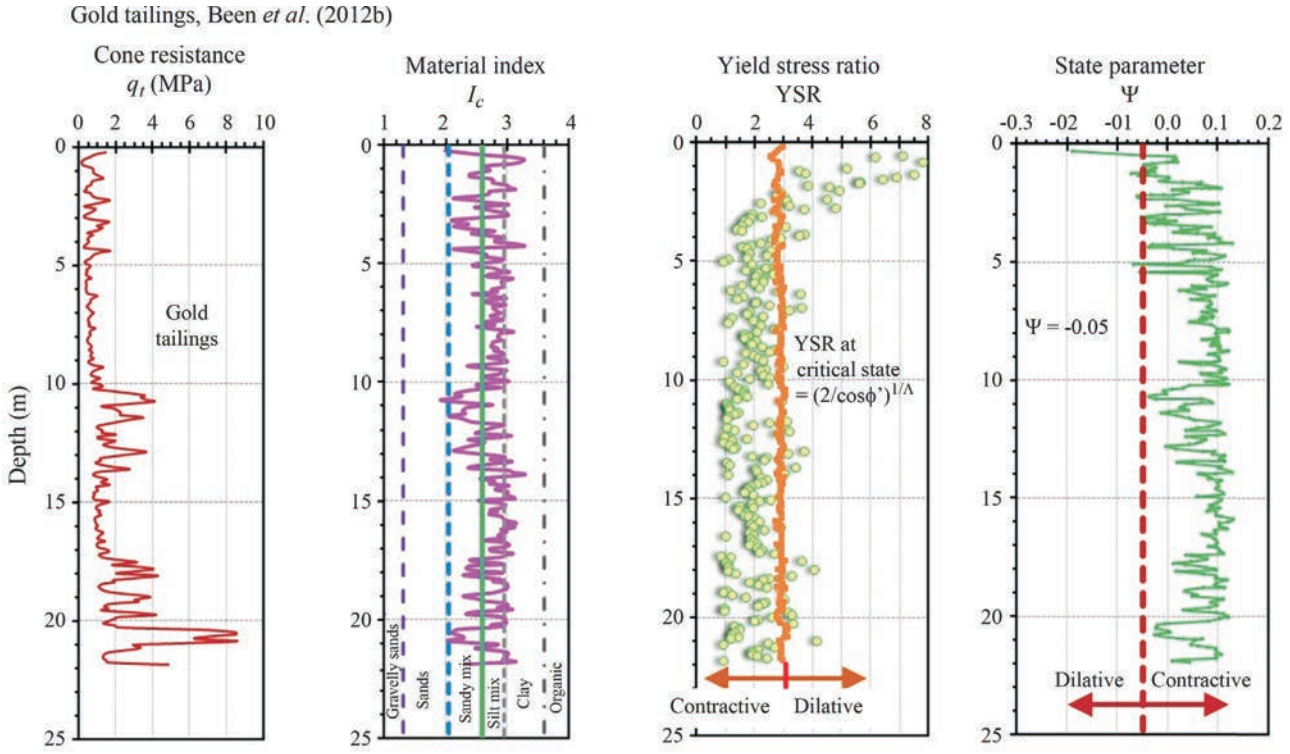

Figure 14 - Flow liquefaction evaluation in gold tailings with profiles: (a) cone resistance, (b) CPT material index, (c) threshold YSR approach, and (d) state parameter (data from Been *et al.*, 2012).

A selected liquefaction case study at Site 19 in Brighton, a suburb of Christchurch, New Zealand that had experienced damages during the 2010-2011 sequences of large earthquakes will be used for illustration. Full details on the liquefaction site are given in Green *et al.* (2014) and a quick summary of the post-processing of the CPTu sounding is presented in Fig. 15. The measured cone tip resistance (q_t) is shown in Fig. 15a with corresponding soil behavior type by CPT index I_c given in Fig. 15b, indicating primarily sands over the 14 m profile, with a shallow silty sand to sandy silt evident in the 2 to 3 m depth range.

Using the YSR_{CSL} threshold clearly shows contractive soil layer in the 2-3 m depths and a thicker critical layer from 6 to 10.5 m. A full cyclic stress-based liquefaction analysis was performed for this site using the standard procedures (Robertson & Wride 1998; Youd *et al.*, 2001). This approach involves a number of steps, including: (a) evaluating of the cyclic stress ratio, CSR; (b) adoption of a threshold triggering curve termed the cyclic resistance ratio, CRR; (b) calculating the stress-normalized cone resistance, Q_{tn}; (c) evaluating CPT index, I_c; (d) correcting the cone resistance to an equivalent value for clean sands, designated: $Q_{tn\text{-}cs}$ based on estimated fines content: $Q_{tn\text{-}cs} = K_c Q_{tn}$. For this site, a moment magnitude M_w = 6.2 and peak ground acceleration PGA = 0.35 g were used in the standard liquefaction procedures to determine the level of ground shaking (*i.e.*, CSR) and the calculated $Q_{tn\text{-}cs}$ profile provided the available soil resistance. This determined the relative profiles of $CSR_{7.5}$ and $CRR_{7.5}$ as shown in Fig. 15d. Green *et al.* (2014) identified sand layer 1 as the critical layer, yet the analyses also showed a thinner and shallower sandy layer that has a high probability of liquefaction. For both layers, the threshold YSR approach clearly recognizes these two sand layers as contractive. Those layers match well with the layers identified by the more rigorous and detailed post-processing procedures.

6.3. Flow liquefaction analysis at Neves Corvo mine, Portugal

Results from CPT and laboratory testing in copper and copper-tin mine tailings at the Neves Corvo mine in southern Portugal are reported by Been *et al.* (2002). Sounding CPT-001 has been post-processed to look at the flow liquefaction potential in these fine-grained tailings, as presented in Fig. 16. The tailings are a special paste fill with cement added to increase stability. Results are shown for the following: (a) cone tip resistance, (b) material index according to Robertson (2009), (c) YSR and threshold value at CSL; (d) state parameter per the Jefferies & Been (2006) type analysis reported by Been *et al.* (2002). For the latter, a zone from 4 to 18 m is indicated to be contractive based on the ψ criterion. Using the YSR criterion, however, a much larger zone of tailings can be considered contractive.

7. Conclusions

A generalized approach to profiling yield stresses in soils from cone penetration tests has been developed from three primary sources: (a) analytical cavity expansion - critical state solution for clays; (b) database of large calibration chamber tests on sands; (c) field and lab data from world-

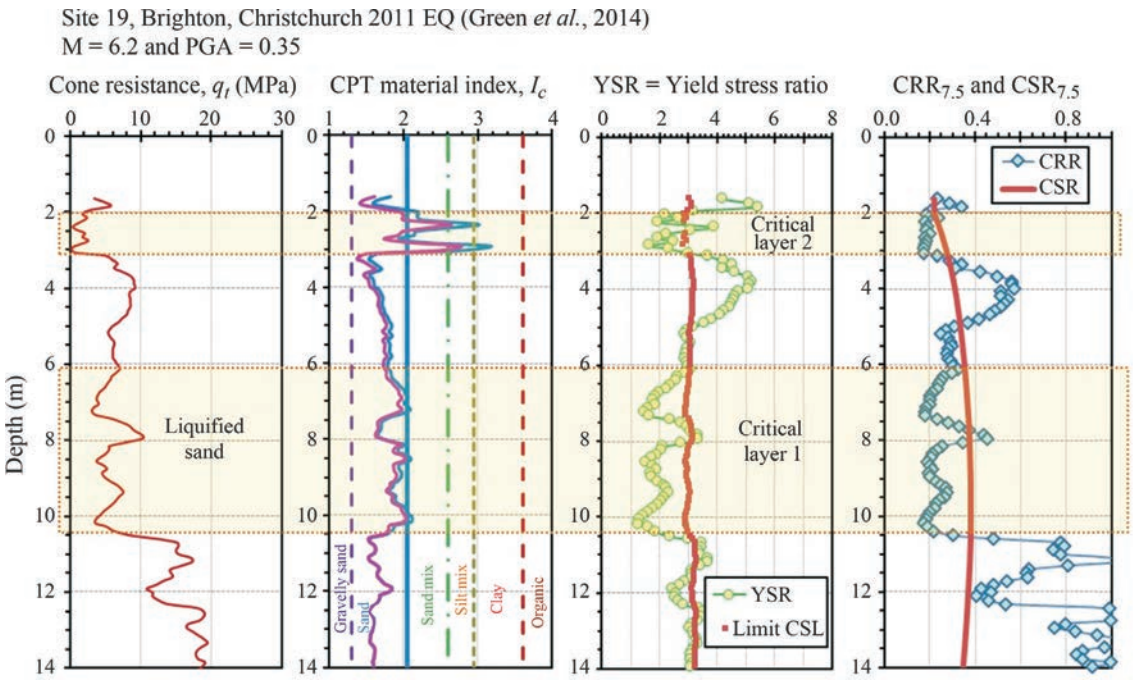

Figure 15 - Cyclic liquefaction case study in natural sands at Site 19, Brighton, Christchurch with profiles: (a) cone resistance, (b) CPT material index, (c) threshold YSR approach, and (d) traditional CRR-CSR comparison (data from Green *et al.*, 2014).

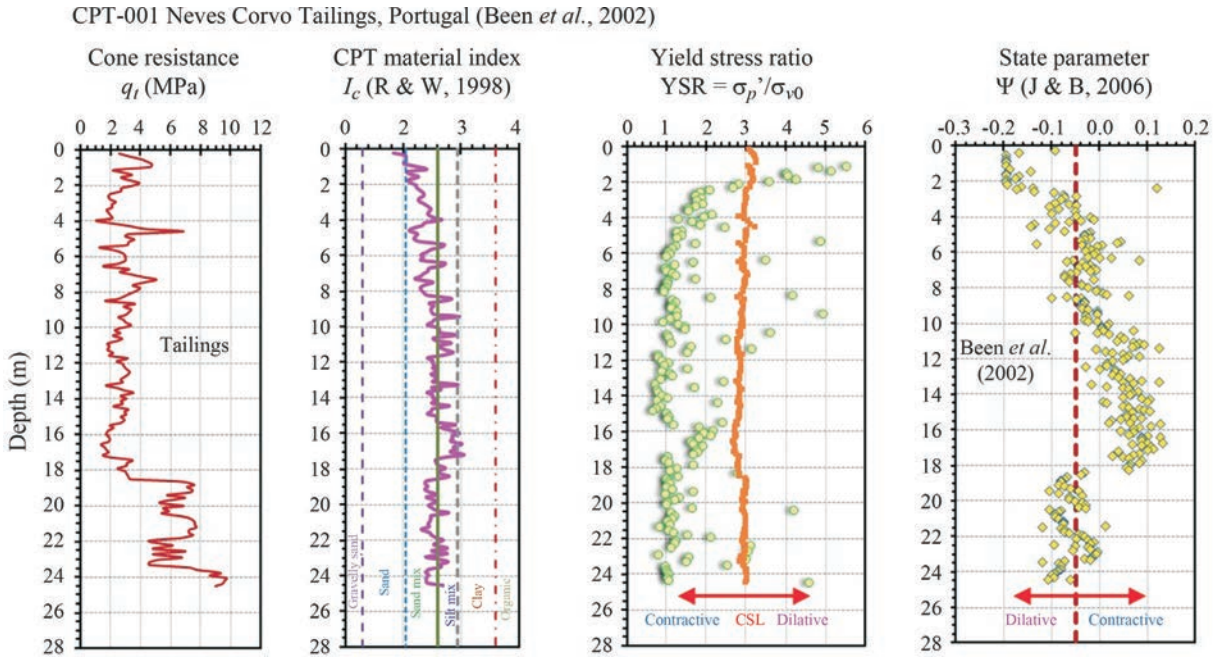

Figure 16 - Flow liquefaction analysis in copper tailings in southern Portugal with profiles: (a) cone resistance, (b) CPT material index, (c) threshold YSR approach, and (d) state parameter (Note: CPT data and interpreted ψ from Been *et al.*, 2002).

wide sites for verification and geoparameter backfitting. In SI units of kilopascal, the yield stress is evaluated simply from $\sigma_p' = 0.33(q_{net})^{m'}$ where the exponent m' tracks well with CPT material index, I_c. The yield stress ratio (YSR = σ_p'/σ_{vo}') demarcates the sorting of normally-consolidated and overconsolidated soils, thus used extensively in embankment and foundation settlement analyses. The YSR also affects the normalized undrained shear strength (s_u/σ_{vo}'), porewater pressures during shear ($\Delta u/\sigma_{vo}'$), soil stiffness (*e.g.*, E_u, G_{max}), as well as the initial state (K_0). Moreover, YSR within a critical state framework can be used to distinguish contractive and dilative soil behavior, thus find application in problems involving flow and cyclic liquefaction.

Acknowledgments

The author appreciates the support of ConeTec Investigations of Richmond, British Columbia and Minnesota Department of Transportation in St. Paul in research activities on cone penetration testing.

References

Agaiby, S. & Mayne, P.W. (2018). Modified SCE-CSSM solution for CPTu soundings in sensitive clays. Paper in preparation. Civil & Environmental Engineering, Georgia Tech.

Baligh, M.M. (1986). Undrained deep penetration: Pore pressures. Geotechnique, 36(4):487-501.

Baroni, M. & Almeida, M.S.S. (2017). Compressibility and stress history of very soft organic clays. Proc. Inst. Civ. Eng. – Geotechnical Engineering, 170(2):148-160.

Been, K.; Jefferies, M.G.; Crooks, J.H.A. & Rothenburg, L. (1987). The cone penetration test in sands: Part II, general inference of state. Geotechnique, 37(3):285-299.

Been, K.; Crooks, J.H.A. & Jefferies, M.G. (1988). Interpretation of Material State From the CPT in Sands and Clays. Penetration Testing in the U.K. Thomas Telford, London, pp. 215-220.

Been, K.; Brown, E.T. & Hepworth, N. (2002). Liquefaction potential of paste fill at Neves Corvo mine, Portugal. Mining Technology, 111(1):47-58.

Been, K.; Romero, S.; Obermeyer, J. & Hebeler, G. (2012). Determining in-situ state of sand and silt tailings from the CPT. Proc. 12th Tailings and Mine Wastes, Keystone, Colorado State University.

Burns, S.E. & Mayne, P.W. (2002). Analytical cavity expansion-critical state model for piezocone dissipation in fine-grained soils. Soils & Foundations, 42(2):131-137.

Casagrande, A. (1936). The determination of the preconsolidation load and its practical significance. Proc. 1st Intl. Conf. on Soil Mechanics & Foundation Engineering, Harvard Univ., Cambridge, v. 3, pp. 60-64.

Casey, B.; Germaine, J.T.; Abdulhadi, N.O.; Kontopoulos, N.S. & Jones, C.A. (2016). Undrained Young's modulus of fine-grained soils. J. Geotechnical & Geoenvironmental Engineering, 1090-0241/04015070.

Chen, B.S-Y. & Mayne, P.W. (1994). Profiling the Overconsolidation Ratio of Clays by Piezocone Tests. Report GIT-CEEGEO-94-1 to National Science Foundation by Georgia Tech Research Corp., Atlanta, 280 p. Download at http://geosystems.ce.gatech.edu/Faculty/Mayne.

Chen, B.S-Y. and Mayne, P.W. (1996). Statistical relationships between piezocone measurements and stress history of clays. Canadian Geotechnical J., 33(3):488-498.

Coutinho, R.Q. & Bello, M.I.M.C.V. (2014). Geotechnical characterization of Suape soft clays, Brazil. Soils & Rocks, 37(3):257-276.

Demers, D. & Leroueil, S. (2002). Evaluation of preconsolidation pressure and the overconsolidation ratio from piezocone tests of clay deposits in Quebec. Canadian Geotechnical Journal, 39(1):174-192.

Diaz-Rodriguez, J.A.; Leroueil, S. & Alem n, J.D. (1992). Yielding of Mexico City clay and other natural clays. Journal of Geotechnical Engineering, 118(7):981-995.

Doherty, P.; Kirwan, L.; Gavin, K. & Igoe, D. (2012). Soil properties at the UCD geotechnical research site at Blessington. Proc. Bridge and Concrete Research in Ireland, Dublin Institute of Technology and Trinity College Dublin, p. 499-504.

Eller, J.M.; McCullough, N.J.; Vargas-Herrera, L.A. & Coto-Loría, M. (2014). Role of CPTu in design of large Atlantic port terminal in Costa Rica. Proc. 3rd IS Cone Penetration Testing, Las Vegas, pp. 1129-1138.

Gavin, K., Cadogan, D., Tolooiyan, A. & Casey, P. (2013). The base resistance of non-displacement piles in sand. Part I. Proc. ICE – Geotechnical Engineering, 166(6):540-548.

Green, R.A.; Cubrinovski, M.; Cox, B.; Wood, C.; Wotherspoon, L.; Bradley, B. & Maurer, B. (2014). Select liquefaction case histories from the 2010-2011 Canterbury earthquake sequence. Earthquake Spectra, 30(1):131-153.

Holtz, R.D.; Kovacs, W.D. & Sheehan, T.C. (2011). An Introduction to Geotechnical Engineering, Second Edition. Pearson Publishing, Upper Saddle River, 864 p.

Idriss, I.M. & Boulanger, R.W. (2008), Soil Liquefaction during Earthquakes. Earthquake Engineering Research Institute, Monograph 12, EERI MNO-12, Oakland, 266 p.

Jamiolkowski, M. & Pepe, M.C. (2001). Vertical yield stress of Pisa clay from piezocone tests. Journal of Geotechnical & Geoenvironmental Engineering, 127(10):893-897.

Jardine, R.J.; Smith, P.R. & Nicholson, D.P. (2003). Properties of the soft Holocene Thames estuary clay from Queensborough, Kent. In: Characterisation and Engineering Properties of Natural Soils. Swets & Zeitlinger, Lisse, v. 1, pp. 599-643.

Jefferies, M. & Been, K. (2006). Soil Liquefaction: A Critical State Approach. Taylor and Francis Group, London, 480 p.

Karlsrud, K.; Lunne, T.; Kort, D.A. & Strandvik, S. (2005). CPTU correlations for clays. Proc. 16th International Conference on Soil Mechanics and Geotechnical Engineering, Osaka, v. 2, pp. 693-702.

Krage, C.P.; Broussard, N.S. & DeJong, J.T. (2014). Estimating rigidity index based on CPT measurements. Proc. 3rd Intl. Symposium on Cone Penetration Testing, CPT'14, Las Vegas, www.cpt14.com.

Ku, T. & Mayne, P.W. (2013). Yield stress history evaluated from paired in-situ shear moduli of different modes. Engineering Geology, 152(1):122-132.

Ladd, C.C. & DeGroot, D.J. (2003). Recommended practice for soft ground site characterization. Soil & Rock America 2003. Proc. 12th Pan American Conference, MIT, Verlag Glückauf Publishing, Essen, v. 1, pp. 3-57.

Larsson, R. & Mulabdic, M. (1991). Piezocone Tests in Clay. SGI Report 42. Swedish Geotechnical Institute, Linköping, 240 p.

Larsson, R. & Åhnberg, H. (2003). Long-term effects of excavations at crests of slopes. SGI Report 61. Swedish Geotechnical Institute, Linköping, 372 p.

Larsson, R. & Åhnberg, H. (2005). On the evaluation of undrained shear strength and preconsolidation pressure from common field tests in clays. Canadian Geotechnical Journal, 42(4):1221-1231.

Larsson, R.; Westerberg, B.; Albing, D.; Knutsson, S. & Carlsson, E. (2007). Sulfidjord. SGI Report 69. Swedish Geotechnical Institute, Linköping, 138 p.

Leroueil, S. & Barbosa, P.S. de A. (2000). Combined effect of fabric, bonding, and partial saturation on yielding of soils. Proc. Unsaturated Soils for Asia, Balkema, Rotterdam, pp. 527-532.

Locat, J.; Tanaka, H.; Tan, T.S.; Dasari, G.R. & Lee, H. (2003). Natural soils: Geotechnical behavior and geological knowledge. Proc. Characterisation & Engineering Properties of Natural Soils. Swets & Zeitlinger, Lisse, v. 1, pp. 3-28.

Long, R.P.; Healy, K.A. & Carey, P.J. (1978). Final report: Field consolidation of varved clay. Univ. Connecticut Report JHR 78-113, Project 70-3 to Connecticut Dept. of Transportation, 162 p.

Mayne, P.W. (1991). Determination of OCR in clays by piezocone tests using cavity expansion and critical state concepts. Soils and Foundations, 31(2):65-76.

Mayne, P.W. (2001). Stress-strain-strength-flow parameters from enhanced in-situ tests. Proc. International Conference on In-Situ Measurement of Soil Properties & Case Histories, Bali, Indonesia, pp. 27-47.

Mayne, P.W. (2005). Integrated ground behavior: In-situ and lab tests. Deformation characteristics of geomaterials. Proc. IS Lyon'03, Taylor & Francis Group, London, v. 2, pp. 155-177.

Mayne, P.W. (2007a). Synthesis 368: Cone Penetration Testing. NCHRP, Transportation Research Board, National Academy Press, Washington, DC, 118 p. www.trb.org.

Mayne, P.W. (2007b). In-situ test calibrations for evaluating soil parameters, characterization & engineering pro-

perties of natural soils. Proc. Singapore 2006, Taylor & Francis Group, London, v. 3, pp. 1602-1652.

Mayne, P.W.; Coop, M.R.; Springman, S.; Huang, A-B. & Zornberg, J. (2009). SOA-1: Geomaterial behavior and testing. Proc. 17th Intl. Conf. Soil Mechanics & Geotechnical Engrg. ICSMGE, Alexandria, Millpress/IOS Press Rotterdam, v. 4, pp. 2777-2872.

Mayne, P.W. (2013). Updating our geotechnical curricula via a balanced approach of in-situ, laboratory, and geophysical testing of soil. Proc. 61st Annual Geotechnical Conference, Minnesota Geotechnical Society, University of Minnesota, St. Paul, pp. 65-86.

Mayne, P.W. (2015). Keynote lecture: In-situ geocharacterization of soils in the year 2016 and beyond. Advances in Soil Mechanics: Geotechnical Synergy. Proc. PCSMGE, Buenos Aires. IOS Press, Amsterdam, v. 5, pp. 139-161.

Mayne, P.W.; Styler, M.; Woeller, D.J. & Sharp, J. (2017). Identifying contractive soils by CPT material index for flow liquefaction concerns. Proc. GeoOttawa - 70th Canadian Geotechnical Conference, Canadian Geotechnical Society: www.cgs.ca.

Mayne, P.W. & Styler, M. (2018). Soil liquefaction evaluation using CPT yield stress profiles and simplified critical state soil mechanics. Proc. Geotechnical Earthquake Engineering and Soil Dynamics V, Austin, TX.

Niazi, F.; Mayne, P.W. & Woeller, D. (2010). Evaluating drilled shaft O-cell response at Golden Ears Bridge from in-situ seismic cone tests. The Art of Foundation Engineering Practice. Proc. Volume in Honor of Clyde Baker (GSP 198), ASCE, Reston, Virginia, pp. 452-469.

Plewes, H.D.; Davies, M.P. & Jefferies, M.G. (1992). CPT-based screening procedure for evaluating liquefaction susceptibility. Proc. 45th Canadian Geotechnical Conference, Paper 4, Toronto, Canadian Geotech Society: www.cgs.ca.

Riyis, M.T. & Giacheti, H.L. (2017). Resistivity piezocone in the conceptual site model definition. Soils & Rocks, 40(2):93-107.

Robertson, P.K. & Wride, C.E. (1998). Evaluating cyclic liquefaction potential using the cone penetration test. Canadian Geotechnical J., 35(3):442-459.

Robertson, P.K. (2009). Interpretation of cone penetration tests: A unified approach. Canadian Geotechnical Journal, 46(11):1337-1355.

Robertson, P.K. (2010). Evaluation of flow liquefaction and liquefied strength using the cone penetration test. J. Geotechnical & Geoenvironmental Engineering, 136(6):842-853.

Robertson, P.K. (2012). The James K. Mitchell Lecture: Interpretation of in-situ tests - Some insights. Proc. Geotechnical & Geophysical Site Characterization 4, Pernambuco, Taylor & Francis Group, London, v. 1, pp. 3-24.

Rodrigues, C.; Amoroso, S.; Cruz, N. & Viana da Fonseca, A. (2016). Liquefaction assessment CPTu tests in a site in south Portugal. Geotechnical & Geophysical Site Characterization 5 (ISC-5), Australian Geomechanics Society, v. 1, pp. 633-638.

Schnaid, F. (2009). In Situ Testing in Geomechanics – The Main Tests. Taylor & Francis, London and New York, 352 p.

Schnaid, F.; Nierwinski, H.P.; Bedin, J. & Odebrecht, E. (2014). On the characterization and classification of bauxite tailings. Soils & Rocks, 37(3):277-284.

Teh, C.I. & Houlsby, G.T. (1991). An analytical study of the cone penetration test in clay. Geotechnique, 41(1):17-34.

Viana da Fonseca, A.; Coop, M.R.; Fahey, M. & Consoli, N.C. (2011). The interpretation of conventional and non-conventional laboratory tests for challenging geotechnical problem. Proc. IS Deformation Characteristics of Geomaterials, Seoul, v. 1, pp. 84-119.

Youd, T.L., Idriss, I., Andrus, R.D., Arango, I., Castro, G., Christian, J.T., Dobry, R., Finn, W.D.L., Harder Jr., L.F., Hynes, M.E., Ishihara, K., Koester, J.P., Liao, S.S.C., Marcuson III, W.F., Martin, J.R., Mitchell, J.K., Moriwaki, Y., Power, M.S., Robertson, P.K., Seed, R.B. & Stokoe, K.H. (2001). Liquefaction Resistance of Soils: Summary Report from the 1996 NCEER and 1998 NCEER/NSF Workshops on Evaluation of Liquefaction Resistance of Soils. Journal of Geotechnical and Geoenvironmental Engineering, 127(10):817-833.